Original Article	*Curr. Appl. Sci.*, **2026**, *4*(1): 1-14 DOI: 10.22034/cas.2025.520327.1048	Current Applied Sciences

Enhancing the Detail Resolution of Foggy Images Using Fuzzy Histogram Equalization with Weighted Distribution

Najme Ghanbari

Department of Electrical Engineering, Faculty of Engineering, University of Zabol, Zabol, Iran

Corresponding author's e-mail: *n.ghanbari@uoz.ac.ir*

Article Information

Received: 30 April 2025
Revised: 31 May 2025
Accepted: 01 June 2025
Published online: 07 June 2025

Keywords

Fuzzy histogram equalization
Weighted distribution
Foggy images
Quality improvement
Gamma correction
Saturation maximization

Abstract

Enhancing image quality is an essential step in developing computer vision since it can significantly increase the efficacy of other algorithms, such as object recognition. Image quality improvement has been done in many different sectors to recover and analyze various aspects. This study combines a weighted fuzzy histogram equalization method with other image quality improvement algorithms to rebuild images affected by inhomogeneous blur. This process begins by generating a phase dissimilarity histogram of the brightness of neighboring pixels to enhance contrast. Gamma correction is then used to boost the dark areas, and maximum saturation is used to prevent the fading effect. The proposed method was evaluated using the PSNR and SSIM indices. These indices are calculated for the results of the proposed method and compared to the previous images. The effectiveness of the proposed algorithm in reconstructing images and the degree to which the results closely resemble the original images will be determined by this comparison. This article also included a qualitative review, the results of which were discussed. Although this method generally sharpens visual details, it might not significantly increase scores in this particular scenario.

1. Introduction

Significant progress has been made in the field of image processing. Notable works have addressed various challenges related to image quality enhancement [1-7]. Fog is a natural phenomenon that reduces visibility and degrades image quality. Visual information retrieval under foggy conditions has received considerable attention in the last decade due to its importance in applications such as autonomous traffic management, driving assistance, and aerial and ground surveillance. One of the main challenges in fog removal techniques is the lack of consistent evaluation standards. Additionally, the limited number of available samples and the scarcity of real foggy image

datasets hinder the training of models and experimental algorithms. This difficulty arises from the challenge of capturing images under identical lighting conditions with and without fog. Many real-world approaches use sophisticated convolutional neural network (CNN) architectures to restore blurry images accurately. However, outputs from these algorithms often suffer from issues such as color fading and blurring. Therefore, it is important to address these problems by integrating multiple previously proposed image enhancement techniques. For example, color augmentation techniques are effective for improving image quality in fields like medical imaging and underwater photography. Unfavorable conditions and poor lighting can negatively affect image quality during capture. For several computer vision applications, factors such as contrast, brightness, and segmentation play crucial roles. Histogram equalization (HE) and gamma correction have been widely used to enhance images taken in low-light environments. However, many of these methods face limitations due to rapid color shifts, maximum saturation, and brightness contrast. Various techniques such as phase transform-based, histogram-based, and HE methods have been developed to improve contrast in low-light images. Despite these developments, many techniques have failed to significantly enhance image clarity in low-light conditions. Nonetheless, HE remains a popular and effective approach for improving color images under such circumstances [8]. The goal of this study is to improve the color quality of erased and reconstructed images so that they more closely resemble the originals. This is achieved through a combination of fuzzy dissimilarity histogram, gamma correction, and saturation maximization. These processes enhance color accuracy and clarity, resulting in final images that appear more natural and lifelike. It is expected that this method will serve as an effective post-processing step for applications such as autonomous vehicles. The primary objectives of this paper are:

1. Implementing the proposed algorithm using Python and evaluating its performance.
2. Assessing the algorithm's effectiveness by measuring PSNR (Peak Signal-to-Noise Ratio) and SSIM (Structural Similarity Index Measure) indices on reconstructed images with inhomogeneous blur.

2. A Review of Past Work

Many HE-based techniques have been put forth in recent decades to improve image quality for improved visual perception [9–13]. To lessen the drawbacks of conventional HE, numerous other HE-based methods have been created, including exposure-based sub-image HE [14] and average sub-image-based cropped HE [15], [16]. Nevertheless, in low light, these techniques do not improve the contrast of color photographs. A generalized equalization model that improves color image contrast while maintaining image quality is shown in [17]. This technique frequently gives dark areas the whole dynamic range, which results in over-enhancement and an unnatural look. For real-time video systems, where clip restrictions lead to insignificant contrast decreases an adaptive, HE with limited contrast is implemented in [18]. Many approaches, from traditional gamma correction to sophisticated strategies utilizing depth picture histograms and textual information, have been put forth to get around these limitations. In contrast to HE-based techniques, an adaptive gamma correction method with weighted distribution is presented in [19] to improve color photographs. However, the previously indicated approach does not maintain the quality of low-light areas. In [20], an ideal gamma correction approach with a weighted sum has been developed to retain brightness while improving contrast. Additionally, a technique known as CLAHE with dual gamma correction was proposed in [21] to improve contrast by increasing brightness. Fuzzy transform-based strategies have been presented in recent years to improve image contrast, surpassing existing methods like the generalized equalization model and traditional HE. A fuzzy logic histogram equalization (FLH) algorithm is

presented in [22] to enhance the contrast of color photographs taken in low light. The FLH algorithm cannot produce much contrast in dark places. In [23], the fuzzy contrast factor is used to create a novel technique for improving the contrast of brightness-preserved photographs. However, in low light, this fuzzy contrast factor-based brightness-preserved method produces undesirable effects. To improve image contrast, a technique known as weighted probability distribution and gamma correction was presented and used in [24]. This technique enhances the input image's contrast while maintaining brightness. To better retain details in images and data, a parametric fuzzy transform method was also introduced in [25]. By retaining the original color and saturation layers, the parametric fuzzy transform PFT successfully maintains the image's naturalness and features. Fuzzy logic also addresses ambiguity and uncertainty in the image histogram. Entropy-preserving mapping is a novel technique for improving the contrast of low-light photos that was proposed in [26]. To enhance the contrast of both color and greyscale images, a novel transform utilizing Gaussian fitting is suggested in [27]. Additionally, [28] presents an evolutionary adaptive gamma correction method that helps maintain the features and brightness of low-contrast photographs. In [29], a novel technique known as local contrast enhancement with adaptive fuzzy exposure is presented to improve the contrast in every area of the image. Also, in [30] a new contrast increase method suggested for dark image. In the future, clustering methods based on fuzzified heuristic algorithms [31] can be used to increase the adaptability of image enhancement methods, especially in the face of regional uncertainty. The idea proposed in [32] can be used to analyze foggy image data. The proposed image enhancement method, based on fuzzy histograms and CNN-based denoising, can potentially be extended to improve data analysis in other domains. For example, it may aid in refining signal estimation in control systems under noise conditions [33] or in enhancing visual inspection of microstructures in material processing applications [34]. Despite these advancements, most prior works either rely on rigid enhancement rules or require preprocessing steps such as clipping or sub-image decomposition, which can lead to detail loss or uneven enhancement. In contrast, the novelty of the present study lies in proposing a weighted fuzzy HE method that omits unnecessary clipping and applies a fuzzy-weighted intensity redistribution strategy. This approach effectively reduces over-brightness while enhancing perceptual image clarity, particularly in non-uniformly blurred and foggy scenes—an area underexplored in the existing literature.

3. Basic Concepts of the Problems

Equation (1) provides a model that can be used to describe a cloudy image. Using a variety of techniques, this equation aids in the reconstruction of the original photos from blurry ones and enhances their quality. In equation (1), A is the general atmospheric light added to the image (a constant value), J(x) is the scene's or the original image's irradiance without the effect of fog, t(x) is the average transmission at point x, and I(x) is the intensity of the image observed at point x under foggy conditions. The value of t(x), which ranges from 0 to 1, indicates how much light makes it through the fog and reaches the camera.

$$I(x)=J(x)t(x)+A(1-t(x)) \quad (1)$$

Recovering A, J(x), and t(x) from I(x) is the overall objective of Dehazing in equation (1). The mathematical models used in traditional Dehazing techniques are derived from prior distributions. One of the popular techniques for image Dehazing is the dark channel approach. This technique is based on the observation that at least one-color channel in a fog-free image has some pixels with extremely low intensity, almost zero. This characteristic is referred to as the "dark channel." After that, a rough transmission map of the fog thickness can be made. Because

their color is typically extremely comparable to ambient light, brighter pixels-like the color of the sky—are utilized as references to generate this channel. Consequently, pixels with higher intensity can be used to determine atmospheric light. Using image fragments, this work shows that haze reduction performs better with greater fragment sizes. However, because fog density does not significantly correspond with image depth, it is challenging to estimate ambient light using standard approaches in inhomogeneous fog photos. Therefore, many recent methods for recovering foggy images involve CNNs rather than classical techniques. In recent years, many variants of these techniques have been created and implemented. To improve response reinforcement, some of these techniques integrate transfer learning with the Res2Net architecture. Some concentrate on improving default methods like channel splitting and the dark channel prior approach, while others employ generative adversarial networks for picture reconstruction. However, none of these methods offer post-processing strategies to enhance areas that convolutional networks have not yet completely addressed. Even when high-scoring models are used for image reconstruction, problems like blurring and color degradation still exist. Since color augmentation greatly enhances visual perception, it is an important field of study in computer vision. HE, for instance, is renowned for its effectiveness and ease of use. Regretfully, under bad lighting conditions, some suggested contrast-boosting techniques do not enhance image quality.

Many HE techniques have been proposed, such as the MMSICHE, CLAHE, GEM, and ESIHE methods. Even though there are many options for color restoration, the methods used today frequently do not improve the contrast of color photos taken in low light or might even make them look strange. This research proposes a novel weighted fuzzy color HE technique to enhance contrast and maintain brightness in input photographs. Adaptive Gamma Correction with Weighted Distribution (AGCWD) works better than conventional HE techniques, according to the data. This algorithm is utilized in the process of eliminating inhomogeneous fog because of its nature. Excessive model complexity is avoided because the paper's goal is to employ CNN and offer the previously discussed method as a post-processing step. Additionally, it stays away from additional post-propagation techniques and intricate network designs. To balance the colors in reconstructed images, this research suggests a novel fuzzy color HE technique.

4. Proposed Method

An outline of the applied approach is given in this section. Although the technique has already been used by others, this study makes important changes to tailor the suggested approach for image processing. To effectively finish the color equalization augmentation, a normalizing step for values between 0 and 255 has also been introduced. The suggested approach is described in detail below. It is assumed that the input image has three RGB color channels (red, green, and blue), each of which has an intensity value $I(x)$ ranging from 0 to 255 (Equation (2)).

$$\mathrm{I(x,y)} = \{\mathrm{R(x,y)}, \mathrm{G(x,y)}, \mathrm{B(x,y)}\} \tag{2}$$

The coordinates of the pixel in the matrix are represented by (x, y) in equation (2). To improve the photographs' color details, color channel stretching is first used. In essence, each color channel is normalized using the greatest (R_{max}) and minimum (R_{min}) intensities. The red channel is precisely defined by equation (3), yielding intensity values ranging from 0 to 1. Due to the fraction's denominator, none of the intensities can be greater than 1 because we are working with minimum and maximum values.

$$R_{em}(x,y) = \frac{R(x,y) - R_{min}}{R_{max} - R_{min}} \tag{3}$$

The image is then converted from the RGB color system to the HSI color space using equations (4), (5), and (6). Similarly, the reverse procedure can be used to convert the HSI color system back to RGB. Assuming that the colors are true and won't change, the method is made to maintain the image's original hues. The normalizing of the input will result in values in the intensity matrix that range from 0 to 1.

$$H = \begin{cases} \cos^{-1} \dfrac{\frac{1}{2} * [(R-G) + (R-B)]}{(R-G)^2 + (R-B) * \sqrt{G-B}} & \text{if } B \le G \\ 360 - \cos^{-1} \dfrac{\frac{1}{2} * [(R-G) + (R-B)]}{(R-G)^2 + (R-B) * \sqrt{G-B}} & \text{if } B > G \end{cases} \tag{4}$$

$$S = 1 - \frac{3}{R+G+B} * [\min(R,G,B)] \tag{5}$$

$$I = \frac{R+G+B}{3} \tag{6}$$

The phase dissimilarity histogram is then computed. The intensity matrix $I(x,y)$ is considered to have $M \times N$ coordinates. The interval $[0, M-1]$ contains the value of x, while the interval $[0, N-1]$ contains the value of y. To map each intensity value according to its neighborhood in a 3×3 grid, the suggested technique first computes a membership function. The suggested algorithm often makes use of 3×3 partitions. Equation (7) defines the membership function. Equation (7) uses the absolute value function since the next step requires calculating the average membership intensity. A lower average is produced if zero is appended to the data rather than utilizing the absolute value. There is no association between the intensities of nearby pixels when the suggested approach is used on images that have already been reconstructed using a Generative Adversarial Network (GAN). To address this issue, the original method lowers the values in this region while potentially increasing and emphasizing some edges. Only the absolute value is set (Equation (7)) rather than the maximum function.

$$\mu(u,v) = \frac{abs(1 - I(x,y) - I(u,v))}{SD} \tag{7}$$

Equation (7) gives us $u = x + i$ and $v = y + j$ for i and j that belong to $[-1,0,1]$. Moreover, SD stands for the original image's standard deviation. The average value of μ in the vicinity of the 3×3 grid is known as $P_{mf}(x,y)$. Since the values fall between 0 and 1, the final membership function cannot be greater than the complement of $P_{mf}(x,y)$. The membership function's final formula is shown in equation (8).

$$\mu_d(x,y) = \left(1 - P_{mf}(x,y)\right) \tag{8}$$

The number of pixels with potential intensities in the interval $[0,255]$ is then used as a conventional histogram structure to compute the histogram of this correlation function. This computation is described in equation (9). The following formula is used to translate intensities between 0 and 255 into values between $[0,1]$. Equation (10), which provides the specifics of this conversion. This conversion entails rounding to the closest integer after multiplying by the maximum intensity value, or 255. Before rounding, a mathematical technique is used to achieve floating-point precision with four decimal places, which increases the conversion accuracy.

$$h_{fd}(p_i) = \sum \sum \mu_d(x,y) \quad for \;\; I(x,y) = p_i \tag{9}$$

$$r(x,y) = \text{int}\left(\frac{\text{int}(I(x,y) \times 1000)}{1000}\right) \times 255 \quad (10)$$

Equation (10), where $I(x,y)$ is the intensity of the original image matrix, $\mu_d\ (x,y)$ is the value of the final membership function, and p_i Is there any conceivable intensity in the interval [0,255] Additionally, the Python method for converting a float to an integer is int, and the intensity transformation for the original matrix's x,y coordinates is $r(x,y)$. The resulting histogram's maximum value will be $h(p_i)$, the scalar size of the $M \times N$ image, because $\mu_d\ (x,y)$ has a value in the interval $[0,1]$. This histogram delivers an average dissimilarity estimate at each intensity level of the input image by interpreting the text data in the vicinity of a pixel. After that, a gamma correction is used to improve the image's dark regions and boost contrast. Histogram slicing, however, may provide an unnatural-looking image because fog-reconstructed images may still contain non-homogeneous fog patches associated with depth. The related cumulative density function (CDF) and probability density function (PDF) are first computed for gamma correction. The formulas for these computations are given in equations (11) and (12), where i stands for any potential intensity in the interval $[0,255]$.

$$\text{PDF(i)} = \frac{\text{h}_{\text{fd}}\ (\text{p}_\text{i})}{\sum_{\text{i}=0}^{255} \text{h}_{\text{fd}}\ (\text{p}_\text{i})} \quad (11)$$

$$CDF(i) = \sum_{j=0}^{i} pdf(j) \quad (12)$$

Equations (11) and (12) are not utilized directly for gamma correction in the suggested approach. Rather, equations (13) and (14) are used to define the weighted histogram distribution and the cumulative weighted distribution function.

$$\text{PDF}_\text{w}\text{(i)} = \text{pdf}_{\text{max}} \times \left(\frac{\text{pdf(i)} - \text{pdf}_{\text{min}}}{\text{pdf}_{\text{max}} - \text{pdf}_{\text{min}}}\right)^{\alpha} \quad (13)$$

$$\text{cdf}_\text{w}\text{(i)} = \sum \frac{\text{pdf}_\text{w}\text{(j)}}{\sum \text{pdf}_\text{w}\text{(j)}} \quad (14)$$

The pdf function's minimum and maximum values are denoted by pdf_{min} and pdf_{max} in equation (13), whereas $\alpha = cdf(i)$. Lastly, equation (15) is used to determine the γ (gamma) value for each intensity. Equation (16) specifies the correction setting for each image intensity.

$$\gamma\text{(i)} = 1 - \text{cdf}_\text{w}\text{(i)} \quad (15)$$

$$\text{I}_\text{e}\text{(x,y)} = \text{i} * \left(\frac{\text{i}}{255}\right)^{\gamma\text{(i)}} \quad (16)$$

The image saturation is improved following $gamma$ correction to the image intensity. To increase image saturation, the following actions are taken:

1. Store the original saturation matrix of the image in HSI space in a new variable.
2. Replace the intensity matrix of the HSI image with the corrected intensity matrix using equation (16).
3. Convert the image from HSI color space to RGB color space.
4. Convert the result back from RGB color space to HSI color space.
5. Each value at the (x,y) coordinates of the original saturation matrix are compared with the corresponding value in the transformation matrix obtained from the previous step. The maximum value between these two is selected to form the final matrix S_{max} representing the maximum saturation matrix.

6. The final corrected image is set as the original Hue matrix, assuming that the maximum saturation matrix and the corrected intensity matrix are correct.
7. If desired, the final result can be converted back to RGB space.

5. Results and Discussion of the Proposed Method

Since the purpose of this paper is to implement and evaluate an algorithm, there is no strict requirement to use a specific training dataset. In this work, a CNN architecture is pre-trained for the task of image denoising. The proposed algorithm subsequently utilizes the denoised images produced by the CNN as its input data. A CNN is employed in this paper to process hazy images and generate their corresponding dehazed approximations. To estimate the optimal transmission map required for image restoration, a dedicated CNN model is designed and trained. The architecture comprises three convolutional layers, each utilizing a distinct filter size to enable multi-scale feature extraction from the input image. The detailed structure of the proposed model is presented below:

```
def create_flatten_layer(layer):
    layer_shape = layer.get_shape()
    num_features = layer_shape[1:4].num_elements()
    layer = tf.reshape(layer, [-1, num_features])
    return layer
def create_fc_layer(input,num_inputs,num_outputs,use_relu=True):
    weights = create_weights(shape=[num_inputs, num_outputs])
    biases = create_biases(num_outputs)
    layer = tf.matmul(input, weights) + biases
    if use_relu:
        layer = tf.nn.relu(layer)
    return layer
layer_conv1=create_convolutional_layer(input=x,num_input_channels=num_channes,conv_filter_size=filter_si
ze_conv1,num_filters=num_filters_conv1)
layer_conv2 = create_convolutional_layer(input=layer_conv1,
 num_input_channels=num_filters_conv1,conv_filter_size=filter_size_conv2,
                                num_filters=num_filters_conv2)
layer_conv3 = create_convolutional_layer(input=layer_conv2,
num_input_channels=num_filters_conv2,conv_filter_size=filter_size_conv3,
                                num_filters=num_filters_conv3)
layer_flat = create_flatten_layer(layer_conv3)
layer_fc1 = create_fc_layer(input=layer_flat,
num_inputs=layer_flat.get_shape()[1:4].num_elements(),
                        num_outputs=fc_layer_size,use_relu=True)
layer_fc2 = create_fc_layer(input=layer_fc1,um_inputs=fc_layer_size,
                        num_outputs=num_classes,use_relu=False)
```

The functionality of CNNs is fundamentally based on the concept of filters and their respective sizes. Filters, also referred to as kernels, play a critical role in CNNs by extracting meaningful features from input data. In these

networks, filters are small matrices that are convolved across the input image, performing localized operations at each position. The size of a filter determines its receptive field, which defines the region of the input image that the filter processes at any given step. For instance, a 3×3 filter analyzes a 3×3 region of the input image during each operation cycle. The subsequent sections describe the roles of the layers employed in the neural network model utilized in this paper. The architecture of the layers is detailed, alongside the presentation of the network's training error. A dataset comprising 477 images was used for training purposes. Although employing larger datasets—such as the NYU2 depth dataset—could potentially enhance performance, the primary objective of proposed method is to develop a model capable of analyzing scattered images collected from diverse sources.

CNN Layer 1: The first layer following the input layer extracts image features using a 3×3 filter, producing a feature map of dimensions 16×14×14. This feature map is subsequently processed through a ReLU activation function.

Slice Layer: The second layer, known as the slice layer, divides the feature map into four separate layers, each with dimensions 4×14×14. This operation facilitates subsequent processing steps, resulting in a feature map with dimensions 4×4×14×14.

Maximum Selection Layer: This layer selects 3D matrices from the feature map and reduces its dimensions back to 4×14×14.

CNN Layer 2: This layer employs the concept of multi-layer mapping to enhance feature extraction from the feature map. The multi-scale hierarchical feature is a scene-level descriptor that exhibits both variation and consistency across the scale space. This property enables the application of broader contextual image information to local recognition decisions, including the identification of appropriately focused and scalable targets, as well as hierarchical natural features. Consequently, this layer provides a solid foundation for the prediction of potential target categories.

CNN Layer 3: The extracted feature map is processed using a CNN layer with a 7×7 filter size in order to reduce information loss and preserve essential features of foggy images. Subsequently, a ReLU activation function is applied to transform the feature map, followed by normalization to scale pixel values between 0 and 1. A collection of generated images is utilized as training samples. By employing Mean Squared Error (MSE) as the loss function, the model minimizes not only the error between the predicted training block and the actual value, but also the error between the residual map and the ground truth. Finally, the neural network model is trained using Stochastic Gradient Descent (SGD) to achieve convergence. Additionally, to ensure experimental reliability, a reasonable number of foggy images were collected from the internet and used to evaluate the model. The resulting test error is illustrated in the figure below (Figure 1).

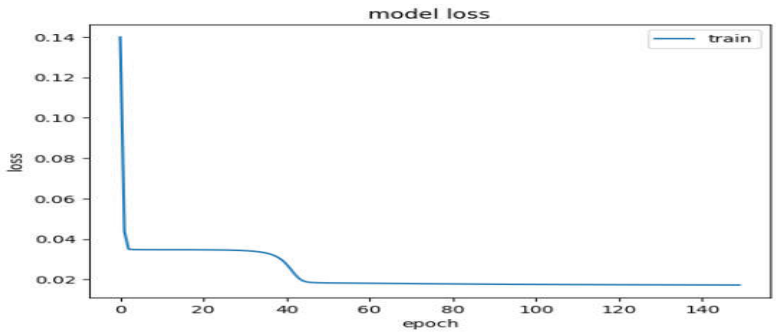

Figure 1. Training error of the proposed neural network model

The suggested approach is used on multiple data samples to precisely compare its performance and outcomes. The Structural Similarity Index (SSIM) and the Peak Signal-to-Noise Ratio (PSNR) are two popular measures for assessing image quality. Equation (17) illustrates how PSNR calculates the difference between the original and reconstructed pictures.

$$\mathrm{PSNR}(f,g) = 10\log_{10}(255^2/\mathrm{MSE}(f,g)) \tag{17}$$

In equation (17) we have:

$$\mathrm{MSE}(f,g) = \frac{1}{MN}\sum_{i=1}^{M}\sum_{j=1}^{N}(f_{ij}-g_{ij})^2 \tag{18}$$

In equation (17), 255 represents the maximum possible pixel value for 8-bit images.

In equation (18), f_{ij} and g_{ij} Denote the pixel values at position (i,j) for the original and resulting images, respectively. M and N represent the dimensions of the image. Instead of measuring pixel-by-pixel differences, the SSIM evaluation criterion assesses the similarity between two images according to human perceptual characteristics. In other words, it focuses on changes in brightness, contrast, and structure. Equations (19) and (20) show how to calculate SSIM for the original image f and the resulting image g. In equation (20), the Mean, Variance, and Covariance values for the images are used. Also, the constants C_1, C_2, and C_3 are constants that prevent division by zero.

$$\begin{cases} L(f,g) = \dfrac{2\mu_f\mu_g + C_1}{\mu_f^2 + \mu_g^2 + C_1} \\ c(f,g) = \dfrac{2\sigma_f\sigma_g + C_2}{\sigma_f^2 + \sigma_g^2 + C_2} \\ s(f,g) = \dfrac{\sigma_{fg} + C_3}{\sigma_f\sigma_g + C_3} \end{cases} \tag{19}$$

In equation (20) we have:

$$\mathrm{SSIM}(f,g) = l(f,g)c(f,g)s(f,g) \tag{20}$$

The evaluation criteria PSNR and SSIM are computed for the test dataset in the suggested approach. The algorithm's input image and the initial histogram distribution are displayed in Figure 2. Parts of the input image are blurry, and some of the edges are not sharply defined. The histogram also reveals that a significant portion of each color channel's pixels are found in high-intensity regions. This suggests that the image is generally brighter and that the colors are not balanced. The algorithm's input fuzzy histogram is displayed in Figure 3. Additionally, the input image's probability distribution function and weighted probability distribution function are displayed in Figures 4 and 5, respectively.

(a)  (b) 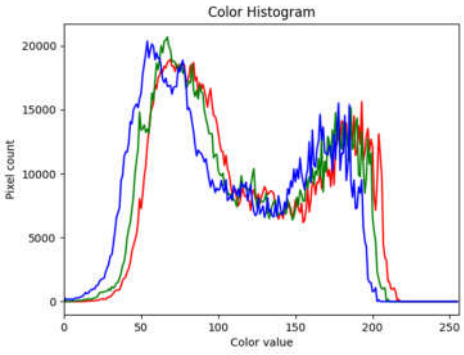

Figure 1. a) Input image b) Histogram distribution

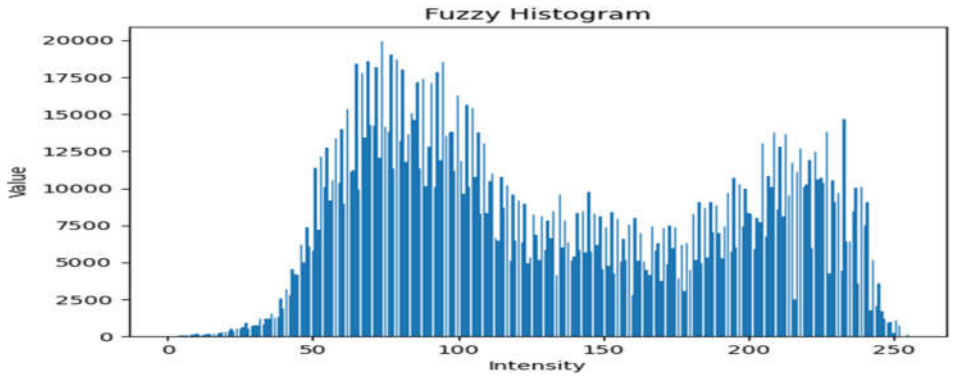

Figure 3. Fuzzy histogram of the algorithm input

Figure 4 shows the probability distribution function and the weighted probability distribution function of the input data. Also, Figure 5 shows the cumulative distribution function and the weighted cumulative distribution function of the input data.

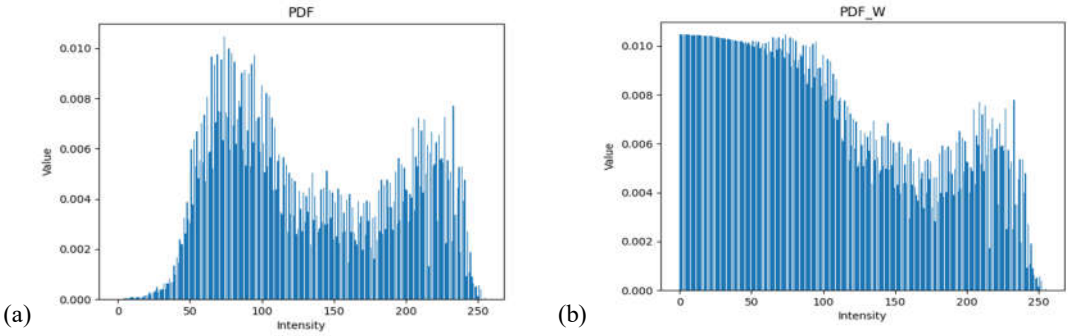

Figure 4. a) Probability distribution function and b) Weighted probability distribution function

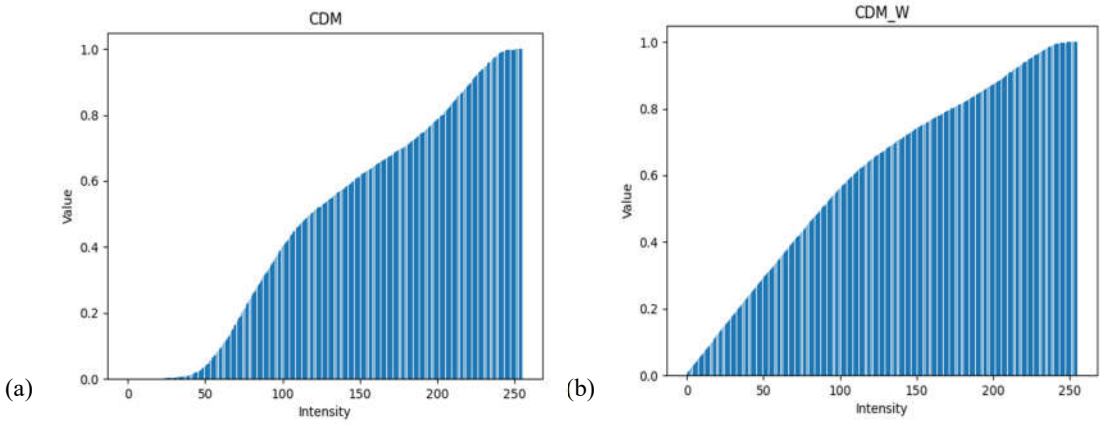

Figure 5. a) Cumulative probability distribution function b) Weighted cumulative probability distribution function

The evolution of the histogram is evaluated at each step of the algorithm. First, it is observed that the shape distribution of the fuzzy histogram is similar to the original histogram. As mentioned, the fuzzy histogram provides a measure of dissimilarity at each intensity level of the 3×3 grid. Similar to the results shown in Figure 3, it is concluded that, on average, there is a large difference between high-intensity pixels. Therefore, it can be said that

the image may exhibit excessive brightness, which usually occurs non-uniformly around neighboring pixels. Furthermore, the probability distribution function (PDF) is expected to resemble the fuzzy histogram in shape, as it assigns a probability (weight) to each mapped intensity. The cumulative histogram shows that most differences in pixel distribution occur at high-intensity values. Because after an intensity value of 100, the probability distribution function (PDF) does not increase by more than 20%. When using weighted distributions, the goal is to maintain brightness while enhancing and enriching the image contrast. Since low-intensity pixels in the input PDF are less likely to be present, the weighted distribution assigns them a higher score. The cumulative probability density function (CDF) is not necessary. Ultimately, each intensity is assigned a score based on its dissimilarity, with high-density distributions being penalized. This idea can be generalized to Figure 5(b). In other words, Figure 5(b) shows a one-to-one linear relationship between intensity values and their probability of occurrence. This represents the ideal behavior, indicating that gamma correction will be performed accurately. Figure 6 shows the final image and its corresponding histogram for each channel. Visually, the edges and some details of the image appear sharper. This is logical because maximizing saturation and increasing contrast improve image clarity. The pixel intensity has also been corrected, and areas with excessive brightness have been removed. In the resulting image, the purity of the colors has enhanced the definition of the image areas. The resulting image histogram tends to preserve the original color distribution. However, the resulting histogram is more balanced compared to the original.

(a)

(b)

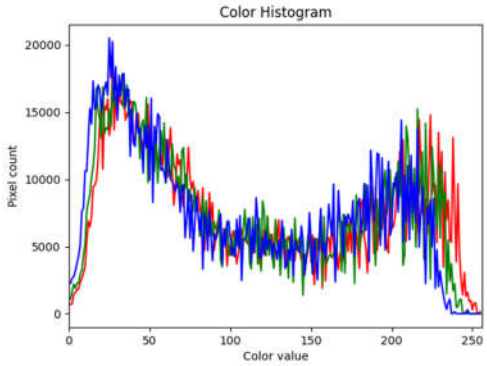

Figure 6. a) Image obtained using the proposed method **b)** Image histogram

In the resulting histogram, low-intensity pixels are present in each of the Three-color channels, and the concentration of high-intensity values has decreased. In other words, the initial input brightness has been modified. It can be concluded that the result obtained is similar to a kind of HE in which the pixels are adjusted within each of the corresponding color channels. Table 1 summarizes the results of evaluating images from the test dataset by calculating the PSNR and SSIM metrics.

The results in Table 1 show that the proposed algorithm has not been successful in improving the SSIM and PSNR scores. This means that the image processed using the proposed method looks less similar to the original image. One possible reason for this could be the more intense effect on the output. Sharpening the image makes the edges and details more visible, but it also makes the defects more visible. In the reconstruction process of the fog removal problem, which is related to the previous step of the proposed method, errors may occur in the image. These errors can include spurious edges or corners, pixel distortion, and unwanted boundary highlighting. The metrics used to compare performance are pixel-based, meaning that any slight change can increase the distance

between actual pixels. The algorithm implemented in this paper enhances the color regions, which may result in image defects becoming more visible, making the image appear less realistic. On the other hand, the proposed algorithm offers the advantage of significantly enhancing edge recovery and reducing blurry patches by increasing the weighted contrast through a fuzzy histogram.

Table 1. PSNR and SSIM metrics from the evaluation of the proposed algorithm

	Before running the algorithm		**After running the algorithm**	
	PSNR	SSIM	PSNR	SSIM
	16.193	0.7059	13.151	0.6266
	24.54900	0.873620	24.642069	0.964715
	14.672497	0.697316	21.351912	0.922074
	15.083771	0.744705	23.069402	0.938261

6. Conclusion

In this paper, a weighted fuzzy histogram algorithm was applied to improve the quality of reconstructed images. This method effectively enhanced image clarity by increasing contrast and reducing haze. Specifically, the proposed approach introduces a novel weighting strategy for histograms by omitting certain steps like clipping, aiming to balance intensities by distributing lower values and penalizing higher ones. Consequently, the algorithm reduces brightness intensity in affected image regions, even when the problem is not uniform across the image. Although quantitative metrics such as PSNR and SSIM decreased, as discussed in the Introduction, there is currently no standard metric for assessing image quality in fog removal tasks. This complicates direct performance comparisons among different methods. Moreover, input images may contain noise or incomplete reconstruction, which can affect evaluation scores as the algorithm may amplify such errors. Despite these challenges, the proposed algorithm successfully enhanced image clarity and enriched details, including edges. It also reduced blurry areas and improved visual sharpness. Since the method is based on, HE and targets intensity recovery, it effectively enhances blurred regions caused by fog.

Acknowledgment

This research was supported by Grant No. IR-UOZ-GR-5366 from the University of Zabol.

Conflicts of Interest

The author declares that there are no conflicts of interest regarding this article.

References

1. Rahimpour N, Azadbakht A, Tahmasbi M, Farahani H, Kheradpishe SR, Javaheri A. Automatic Cadastral Boundary Detection of Very High-Resolution Images Using Mask R-CNN. *J. Electr. Comput. Eng. Innov.* 2024, 12(2), 525-534.
2. Fooladi S, Farsi H, Mohamadzadeh S. Segmentation of Skin Lesions in Dermoscopic Images Using a Combination of Wavelet Transform and Modified U-Net Architecture. *J. Electr. Comput. Eng. Innov.* 2025, 13(1), 1511168.
3. Talouki AG, Koochari A, Edalatpanah S A. Applications of Neutrosophic Logic in Image Processing: A Survey. *J. Electr. Comput. Eng. Innov.* 2022, 10(1), 243-258.
4. Sabeti V. An Improved Approach to Blind Image Steganalysis Using an Overlapping Blocks Idea. *J. Electr. Comput. Eng. Innov.* 2023, 11(2), 263-276.
5. Tabahfar HK, Mahmoudi FT. Optimum Spectral Indices for Water Bodies Recognition Based on Genetic Algorithm and Sentinel-2 Satellite Images. *J. Electr. Comput. Eng. Innov.* 2024, 12(1), 217-226.
6. Taheri M, Rastgarpour M, Koochari A. A Novel Method for Medical Image Segmentation Based on Convolutional Neural Networks with SGD Optimization. *J. Electr. Comput. Eng. Innov.* 2021, 9(1), 37-46.
7. Masoudifar M, Pourreza HR. Depth Estimation and Deblurring from a Single Image Using an Optimized-Throughput Coded Aperture. *J. Electr. Comput. Eng. Innov.* 2023, 11(1), 51-64.
8. Dorothy R, Joany RM, Rathish RJ, Prabha SS, Rajendran S, Joseph ST. Image enhancement by histogram equalization. *Int. J. Nano Corros. Sci. Eng.* 2015, 2(4), 21-30.
9. Mayathevar K, Veluchamy M, Subramani B. Fuzzy color histogram equalization with weighted distribution for image enhancement. *Optik* 2020, 216, 164927.
10. Mustafa WA, Abdul Kader MM. A Review of Histogram Equalization Techniques in Image Enhancement Application. *J. Phys. Conf. Ser.* 2018, 1019(1), 012026.
11. Seddighi S. Improving image quality using multi-part histogram and histogram slicing. *In* Second Conference on Computer and Network Technology Perspectives in 2030. 2016.
12. Lin SC, Wong CY, Rahman MA, Jiang G, Liu S, Kwok N, Shi H, Yu YH, Wu T. Image enhancement using the averaging histogram equalization (AVHEQ) approach for contrast improvement and brightness preservation. *Comput. Electr. Eng.* 2015, 46, 356-370.
13. Kumar P. Image enhancement using histogram equalization and histogram specification on different color spaces (PhD dissertation). 2014.
14. Singh K, Kapoor R. Image enhancement using Exposure based Sub Image Histogram Equalization. *Pattern Recognit. Lett.* 2014, 36, 10-14.
15. Singh K, Kapoor R. Image enhancement via Median-Mean Based Sub-Image-Clipped Histogram Equalization. *Optik* 2014, 125(17), 4646-4651.
16. Zarie M, Hajghassem H, Eslami Majd A. Image Contrast Enhancement Using Triple Dynamic Clipped Histogram Equalization. *Tabriz J. Electr. Eng.* 2018, 48(2), 667-77.
17. Xu H, Wang R, Shu Z. Xu A. On the convergence of approximating tensor-product rational Bézier surfaces using tensor-product Bézier surfaces. *J. Approx. Theory* 2014, 182, 68-82.
18. Yadav G, Maheshwari S. Agarwal A. Contrast limited adaptive histogram equalization-based enhancement for real time video system. *In* 2014 International Conference on Advances in Computing, Communications and Informatics (ICACCI). 2014, 2392-2397.

19. Huang SC, Cheng FC, Chiu YS. Efficient Contrast Enhancement Using Adaptive Gamma Correction with Weighting Distribution. *IEEE Trans. Image Process.* 2013, 22(3), 1032-1041.

20. Jiang G, Wong CY, Lin SC, Rahman MA, Ren TR, Kwok N, Shi H, Yu YH, Wu T. Image contrast enhancement with brightness preservation using an optimal gamma correction and weighted sum approach. *J. Mod. Opt.* 2015, 62, 1-12.

21. Chang Y, Jung C, Ke P, Song H, Hwang J. Automatic Contrast-Limited Adaptive Histogram Equalization with Dual Gamma Correction. *IEEE Access* 2018, 6, 11782-11792.

22. Raju G, Nair MS. A fast and efficient color image enhancement method based on fuzzy-logic and histogram. *AEU Int. J. Electron. Commun.* 2014, 68(3), 237-243.

23. Hasikin K, Mat Isa NA. Adaptive fuzzy contrast factor enhancement technique for low contrast and nonuniform illumination images. *Signal Image Video Process.* 2012, 8(8), 1591-1603.

24. Gupta B, Tiwari M. Minimum mean brightness error contrast enhancement of color images using adaptive gamma correction with color preserving framework. *Optik* 2016, 127(4), 1671-1676.

25. Chandrasekharan R, Sasikumar M. Fuzzy Transform for Contrast Enhancement of Non-uniform Illumination Images. *IEEE Signal Process. Lett.* 2018, 25(6), 813-817.

26. Chen BH, Wu YL, Shi LF. A Fast Image Contrast Enhancement Algorithm Using Entropy-Preserving Mapping Prior. *IEEE Trans. Circuits Syst. Video Technol.* 2017, 29(1), 38-49.

27. Sun X, Xu Q, Zhu L. An Effective Gaussian Fitting Approach for Image Contrast Enhancement. *IEEE Access* 2019, 7, 31946-31958.

28. Mahmood A, Khan S, Hussain S, Almaghayreh E. An Adaptive Image Contrast Enhancement Technique for Low-Contrast Images. *IEEE Access* 2019, 7, 161584-161593.

29. Jirjees A, Hasikin K, Mat Isa NA. Adaptive Fuzzy Exposure Local Contrast Enhancement. *IEEE Access* 2018, 6, 58794-58806.

30. Alavi M, Kargari M. A new contrast enhancement method for Color dark and low-light images. *In* 2022 9th Iranian Joint Congress on Fuzzy and Intelligent Systems (CFIS). 2022, 1-7.

31. Ghanbari N, Zahiri SH, Shahraki H. Clustering of Triangular Fuzzy Data Based on Heuristic Methods. *J. Electr. Comput. Eng. Innov.* 2024, 12(1), 1-14.

32. Ghanbari N, Zahiri SH, Shahraki H. Clustering of Fuzzy Data Sets Based on Particle Swarm Optimization With Fuzzy Cluster Centers. *Int. J. Ind. Eng. Prod. Res.* 2022, 33(2), 1-2.

33. Pourmir M. Optimization of the State of an Inverted Pendulum System Using Kalman Filter in the Presence of Gaussian and Poisson Noise. *Curr. Appl. Sci.* 2025, 3(2), 61-72.

34. Kaykha M. M. Effect of Constrained Studded Pressing on the Microstructure and Residual Stresses for Producing Nanostructure Pure Copper Sheet. *Curr. Appl. Sci.* 2025, 3(1), 47-56.

How to cite this article: Ghanbari N. Enhancing the Detail Resolution of Foggy Images Using Fuzzy Histogram Equalization with Weighted Distribution. *Curr. Appl. Sci.*, 2026, 4(1):1-14. https://doi.org/10.22034/cas.2025.520327.1048